

SUCCESSFUL APPLICATION OF CERAMIC POROUS WICK IN LOOP HEAT PIPE AND CAPILLARY PUMPING LOOP

Paulo Henrique Dias dos Santos, paulosantos@labcet.ufsc.br

Rafael Branco dos Santos, rafaelsantos85@gmail.com

Lucas Freitas Berti, berti@labcet.ufsc.br

Edevaldo Brandilio Reinaldo, edevaldo@emc.ufsc.br

Eduardo Gonçalves Reimbrecht, eduardo@labcet.ufsc.br

Edson Bazzo, ebazzo@emc.ufsc.br

Federal University of Santa Catarina, Department of Mechanical Engineering, LabCET - Laboratory of Combustion and Thermal Systems Engineering, Campus Universitário, 88.040-900, Florianópolis, SC, Brazil

Abstract. *Most porous structures used in Loop Heat Pipes (LHP) and Capillary Pumping Loop (CPL) have been made of metallic material, such as nickel, titanium and stainless steel. Metallic wicks have low thermal resistance and allow a considerable amount of heat from evaporation zone to the inlet liquid channel, leading to bubbles formation and blocking the liquid feeding channel. Moreover, the machining process of porous metal structures can block the external pores and hence reduce the liquid flow. The use of ceramic wick can minimize the problems of bubble formation and pores obstruction. In this paper, three capillary pumping systems, one LHP and two CPLs, were tested in order to evaluate the thermal performance and applicability of these systems in thermal control of microprocessors and electronic components in general. The LHP has one assembly composed by one capillary evaporator and one compensation chamber. This assembly is cylindrical with 65 mm of length and 10 mm of diameter. The evaporator active zone has 25 mm of length. One of the CPLs has a flat capillary evaporator with diameter of 30 mm and height of 10mm. The other one is cylindrical with length of 85 mm and 15 mm of diameter. Acetone was used as working fluid. Ceramic porous wicks are proposed as alternative to wicks made of metallic material. The experimental results of the capillary pumping systems have demonstrated a successful application of ceramic porous wicks in these devices. The tests have shown a successful start up and steady state operation.*

Keywords: *Ceramic porous wick, LHP, CPL.*

1. INTRODUCTION

CPL and LHP are two-phase heat transfer loops currently in development for aerospace and refrigeration systems applications. Ammonia, water and acetone have been used as the working fluid, usually defined according the operation temperature. The capillary pressure is the driven force which makes the working fluid to circulate through the loop. The wick structure placed into the evaporator is responsible to provide capillary pressure. No pumping mechanism or electric power is required to circulate the working fluid.

Metallic, polymeric and ceramic materials have commonly been used as wick structure. A successful application of ceramic porous wick in capillary pumping systems is the main goal of this paper. The proper fitting of the capillary structure inside the envelope evaporator is the first challenge to be overcome. The assemble is relatively complex because the metallic envelope requires close contact tolerances at the interface between envelope walls and wick surface. This contact should be fit in order to minimize the thermal resistance and any vapor leak back to the liquid channel.

In order to obtain close tolerances, a machining process is required for these wick structures. However, machining process of metallic wick structure is not easy, because the possibility of open porosity obstruction due to the plastic deformation. On the other hand, ceramic wick structure does not present plastic deformation during the machining process. Furthermore, when a material is designed to be porous the particles do not consolidate harder as a dense material. Therefore, the ceramic wick structure can be machined by conventional machining process and the open porosity remains the same, Janssen (2008).

In this work, special attention is also focused on the heat transfer processes and thermodynamic behavior of both, the CPL and LHP. Ku (1994) was the first to report a real conditions evaluation of CPL

operation, basing his analysis on the PT diagram. A similar analysis, through the PT diagram, was also published for LHP by Maidanik et al. (1991), Ku (1999) and Maidanik (2004). The operation modes of the capillary pumping systems can be classified as fixed or variable conductance mode. In the variable conductance mode, the operation temperature can be controlled even for thermal load changing. On the other hand in case of fixed conductance mode, the greater the thermal load, the greater the operation temperature. Nikitkin and Cullimore (1998) reported qualitative graphs of the vapor temperature profile for CPL and LHP operating in the fixed and variable conductance modes. Furthermore, Chernysheva et al. (2007) just presented quantitative graphs for LHP.

In this paper, three capillary pumping systems, one LHP and two CPLs, were tested in order to evaluate the thermal performance and applicability in thermal control of microprocessors and electronic components in general. Ceramic porous wicks are proposed as alternative to wicks made of metallic materials. All evaporators of the capillary pumping systems under study used ceramic wicks. Experimental results concerning this application in one LHP and two CPLs are presented. The LHP has one assembly composed by one capillary evaporator and one compensation chamber. This assembly is cylindrical with 65 mm of length and 10 mm of diameter. The evaporator active zone has 25 mm of length. One of the CPLs has a flat capillary evaporator with diameter of 30 mm and height of 10mm. The other CPL has a cylindrical evaporator with length of 85 mm and 15 mm of diameter. Acetone was used as working fluid. The paper also presents an introduction to the thermohydraulic study in regard to the CPL/LHP design, the fixed and variable conductance modes and the Pressure-Temperature diagrams for CPL/LHP.

2. OPERATION MODES

2.1. Fixed Conductance

The operation modes of the capillary pumping systems can be classified as fixed or variable conductance. Fig. 1 depicts a typical fixed conductance CPL. This device is composed of an evaporator, a condenser, a subcooler and liquid and vapor transport lines. A working fluid evaporates when heated into the evaporator and condenses when cooled into the condenser. The fluid flows continuously in a same direction, differently of heat pipes, where the liquid and the vapor flow in opposite directions.

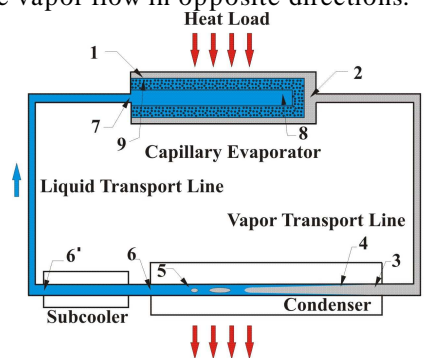


Figure 1. Functional schematic of a fixed conductance CPL.

Fixed conductance CPL operates in the following manner: heat is supplied to the evaporator so that the liquid saturated into the wick evaporates, forming at the same time the menisci in the interface liquid-vapor, that promote the fluid circulation through the capillary forces developed by the fluid surface tension. The vapor generated in the evaporator goes via vapor transport line to the condenser, where heat is removed and the vapor condenses. The fluid is subcooled before coming back to the evaporator so that no vapor bubble migrates to the evaporator.

Fixed conductance CPLs have as characteristics: (i) they do not have reservoir for fluid storing; (ii) the subcooler is usually part of the condenser; (iii) the vapor condensation area remains constant even for thermal load variation. Therefore, the operation temperature depends on the thermal load supplied to the evaporator and on the condenser sink temperature. The maximum capillary pressure head ($\Delta P_{cap,max} [Pa]$) is function of the fluid surface tension ($\sigma [N/m]$), the effective pumping radius of the wick ($r_p [m]$) and the contact angle between the liquid and the vapor phase ($\theta = 0^\circ$):

$$\Delta P_{cap,max} = \frac{2\sigma \cos \theta}{r_p} \quad (1)$$

The CPL operation requires that the sum of the pressure drops in the components and transport lines must be smaller than the maximum capillary pressure head developed by the wick:

$$\Delta P_{cap,max} \geq \Delta P_{evap} + \Delta P_{cond} + \Delta P_v + \Delta P_l + \Delta P_g \quad (2)$$

A PT diagram is depicted in Fig. 2 for better understanding the CPL phenomena (see also Fig. 1). In order to simplify the discussion, it is assumed that the transport lines are not insulated. In the point 1, the liquid vaporizes at a saturation temperature T_1 corresponding to a pressure P_1 . The generated vapor flows through the evaporator grooves causing a pressure drop due to the viscous friction from P_1 to P_2 , in a close location of the evaporator outlet, where liquid vaporizes at a lower saturation temperature T_2' . Therefore, the liquid vaporizes along the external wick surface at a temperature range between T_1 and T_2' , instead of a fixed temperature T_1 . The vapor leaves the evaporator in the superheated state (point 2) partly due to the decrease in the saturation pressure and partly due to the proximity of the hot source that supplies the system. The vapor continues to lose pressure as flows via vapor transport line. Between the points 2 and 3, the vapor experienced an expansion process and its temperature decreases lightly.

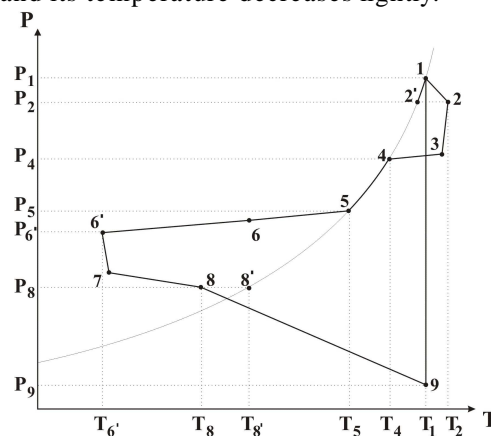


Figure 2. PT diagram for a fixed conductance CPL.

The vapor thermodynamic state that enters in the condenser is represented by the temperature T_3 and pressure P_3 . According to Ku (1994) a small area of the condenser is enough to dissipate the sensible heat before the beginning of the vapor condensation in the point 4 at a pressure P_4 (smaller than P_3) and at a saturation temperature T_4 .

The vapor condensation happens between the points 4 and 5. In the point 5 there is no more vapor. Similar to the liquid vaporization into the evaporator, the vapor condensation occurs at a temperature range between T_4 e T_5 . The liquid continues to lose sensible heat up to reach a subcooled temperature T_6 in the condenser outlet. A further subcooling is necessary to ensure that no vapor bubble goes to the evaporator. Therefore the liquid goes by the subcooler and leaves it in a subcooling state to the temperature T_6' . The liquid temperature increases lightly, while the pressure decreases from P_6' to P_7 in the liquid feeding channel inlet of the evaporator. Inside the feeding channel, the liquid is heated until a temperature T_8 . This heating is due to the heat leak from the wick to the fluid.

The point $8'$ represents the saturation state corresponding to the pressure P_8 . The liquid in the external wick surface is heated and reaches the saturation temperature T_1 corresponding to the pressure P_1 before vaporizing. It is noticed by Fig. 2 that the liquid side of the menisci (point 9) is in its superheated state. The total pressure drop in the system is equal to the difference between P_1 and P_9 which in its turn cannot be larger than the maximum capillary pressure head. According to Ku (1999), in the most of the two-phase

capillary pumping systems the changes of pressure and temperature are extremely small; therefore it can approach the saturation curve for a straight line between two points using the Clausius-Clapeyron equation:

$$\left. \frac{dP}{dT} \right|_{T_{sat}} = \frac{h_{lv}}{T_{sat} v_{lv}} \quad (3)$$

where: $\left. \frac{dP}{dT} \right|_{T_{sat}}$ is the slope of the pressure-temperature saturation line $[Pa/K]$, h_{lv} is the latent heat of vaporization $[kJ/kgK]$, T_{sat} is the saturation temperature $[K]$ e v_{lv} is the difference in specific volumes during vaporization $[m^3/kg]$.

According to Maidanik et al. (1991), taking for instance the points 1 and 4, the saturation line slope times the temperature differential between these two points of the curve is approximately equal to the pressure differential between them:

$$\left. \frac{dP}{dT} \right|_{T_i} (T_1 - T_4) \approx (P_1 - P_4) \quad (4)$$

In Eq. (4), is noticed that the decrease in the temperature is directly proportional to the pressure drop between the points 1 and 4. This pressure drop is function of the mass flow rate which in its turn is function of the power input to the evaporator.

According to Ku (1994), the heat transfer rate by vaporization is the same that by condensation ($\dot{Q}_{cond} = \dot{Q}_{evap} [W]$). The heat transfer rate in the condenser can be expressed as:

$$\dot{Q}_{cond} = h_{cond} A_{cond} (T_4 - T_0) \quad (5)$$

where: h_{cond} is the heat transfer coefficient $[W/m^2K]$ and A_{cond} is the heat transfer area $[m^2]$ in the condenser.

For a CPL with fixed liquid volume, the thermal conductance ($h_{cond} A_{cond}$) remains constant. For a given heat transfer rate rejected by the condenser (\dot{Q}_{cond}) and a condenser sink temperature T_0 , the vapor in the condenser will condense at the temperature T_4 in agreement with Eq. (5) and the liquid will vaporize in the evaporator at the temperature T_1 in agreement with Eq. (4).

Any change in the input heat to the evaporator and/or in the condenser sink temperature will result in changes of the T_1 and T_4 . Therefore, the main characteristic of a fixed conductance CPL is its strongly dependence on the operation temperature with regard to the input heat and to the condenser sink temperature.

2.2. Variable Conductance

In a variable conductance CPL, a reservoir will be included. The reservoir function is to control the operation temperature of the system and to accumulate the liquid excess that is not being required in the loop.

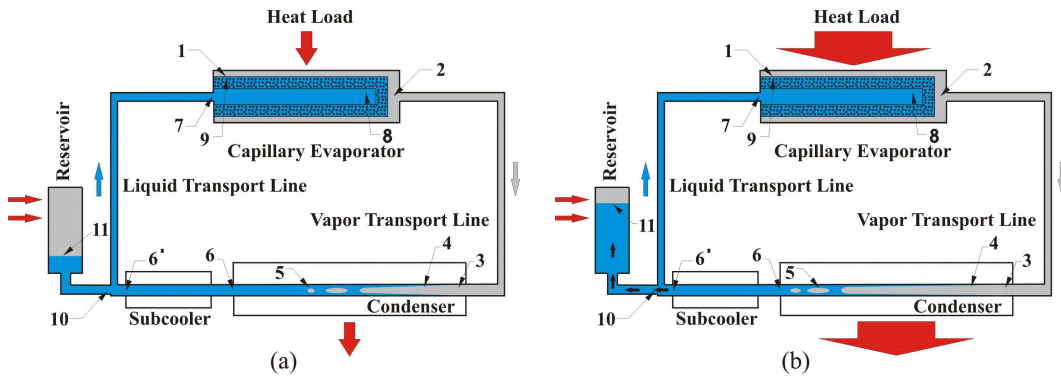


Figure 3. Functional schematic of a variable conductance CPL.

Analyzing Eq. (5), can be understood how works the variable conductance mechanism. If the condenser sink temperature T_0 remains constant and the system thermal load increases, more vapor will be generated in the evaporator and the vapor excess will accumulate in the condenser, causing a local pressure increase. This pressure increase which in its turn causes a liquid displacement from the condenser to the reservoir, as it can be seen in Fig. 3.

This happens because the condensation temperature T_4 remains constant and the heat transfer area A_{cond} increases so that Eq. (5) is satisfied. In case the system thermal load decreases and T_0 remains constant, the vapor pressure into the condenser will decrease. An unbalance in the pressure between the reservoir and the condenser will force the liquid displacement from the reservoir to the condenser, reducing the heat transfer area A_{cond} automatically so that Eq. (5) is satisfied. Similar analysis can be made varying the condenser sink temperature T_0 . The Fig. 4 depicts a PT diagram for a variable conductance CPL, shown in Fig. 3. The point 11 corresponds to the saturation state into the reservoir. In any circumstance, the vapor condensation temperature T_4 is related to the reservoir saturation temperature T_{11} by the union of Eqs. (3 and 4):

$$(T_4 - T_{11}) = \frac{(P_4 - P_{11})T_{11}v_{lv}}{h_{lv}} \quad (6)$$

The PT diagram is developed for steady state; therefore there is no mass flow between the loop and the reservoir. The only pressure gradient possible between the points 10 and 11 is due to the hydrostatic pressure. The other points are similar to the ones showed in Fig. 2.

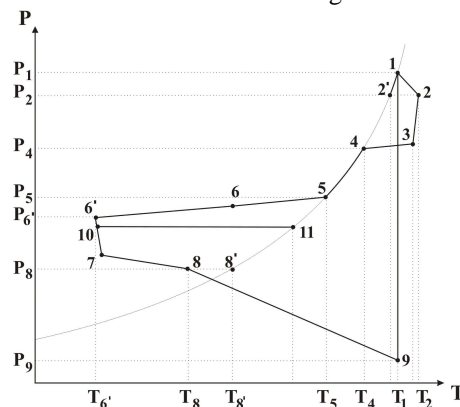


Figure 4. PT diagram for a variable conductance CPL.

The variable conductance CPL, shown in Fig. 3, operates in the following manner: before the system startup, the condenser is submitted to the temperature T_0 and the reservoir is heated up to temperature T_{11} (which is higher than the temperatures of the rest of the loop). Then, the thermal load is supplied to the evaporator. As the evaporator is heated up to the same temperature T_{11} or lightly superior to the one, the liquid is vaporized and the menisci formed in the wick force the vapor flowing to the condenser via vapor transport line. An equilibrium condition will be established in the condenser so that the vapor condenses at the temperature T_4 that is very close to the reservoir temperature T_{11} . An equilibrium condition will also be established in the evaporator so that the liquid vaporizes to the temperature T_7 . The condensation temperature T_4 is not sensitive nor to the changes in the condenser sink temperature T_0 , much less to the changes in the system thermal load. Therefore, the temperature T_4 is controlled by the reservoir saturation temperature T_{11} .

LHP is a type of variable conductance CPL and was developed to supply the apparent disadvantage of CPL in the needed of pre-heating during the startup. In LHP, the reservoir, also denominated hydro-accumulator or compensation chamber which has capillary connection with the evaporator, ensures the liquid presence in the evaporator wick. A secondary wick usually connects the compensation chamber to the evaporator. The compensation chamber is located close to the evaporator, usually in the capillary pumping inlet as it can be seen in Fig. 5; or taking the place of what would be the liquid feeding channel of the evaporator. Thereby, in a LHP the liquid reservoir presents direct thermal contact with the evaporator (hot

source), differently of CPL where it is connected to the condenser (cold source). The Fig. 6 depicts a PT diagram for variable conductance LHP, shown in Fig. 5. The point 10 corresponds to the saturation state into the compensation chamber. In any circumstance, the liquid vaporization temperature T_l is related to the saturation temperature of the compensation chamber T_{l0} by the union of Eqs. (3 and 4):

$$(T_l - T_{l0}) = \frac{(P_l - P_{l0})T_{l0}v_{lv}}{h_{lv}} \quad (7)$$

The PT diagram, shown in Fig. 6, presents an analysis for steady state; therefore there is no mass flow between the compensation chamber and the liquid feeding channel of the evaporator. Consequently, the saturation pressure P_{10} in the compensation chamber should be the same pressure P_7 . The capillary pumping systems in the variable conductance mode (CPL and LHP shown in Figs. 3 and 5) can work in a binary operation mode.

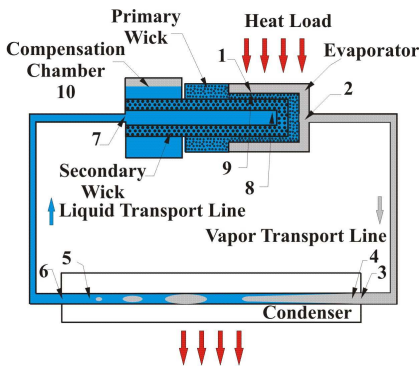


Figure 5. Functional schematic of a LHP.

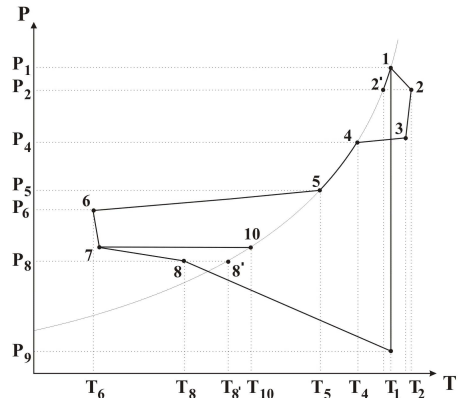


Figure 6. PT diagram for a LHP.

When these systems are operating in a low thermal load condition, the reservoir (CPL) or the compensation chamber (LHP) are operating in the two-phase condition. As it was already mentioned, when the thermal load increases, the condensation front moves forward, causing the liquid displacement from the condenser to the reservoir (CPL) or to the compensation chamber (LHP). Therefore, as the thermal load increases, these compartments will be filled out by the liquid in excess and there will be no more two-phase condition. The evaporation temperature control is only possible if the liquid compartment of the system is in two-phase condition. Consequently, if the thermal load increases up to whole filling of the reservoir (CPL) or the compensation chamber (LHP), the saturation temperature control of the system cannot be made.

Fig. 7 shows qualitatively how is the evaporation temperature profile as a function of the thermal load of CPL and LHP that work in the binary operation mode (fixed and variable conductance). Fig. (7a) depicts that the evaporator temperature of CPL remains constant in the variable conductance operation mode and starts to increase linearly in the fixed conductance mode.

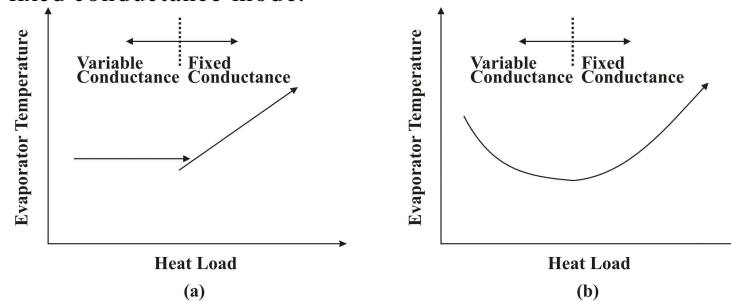


Figure 7. Typical curves of operation for CPL (a) and for LHP (b) in the fixed and variable conductance (Nittkin and Cullimore, 1998).

While for LHP, Fig. (7b), even operating in the variable conductance operation mode the evaporator temperature does not remain constant. LHP possesses a range of the evaporation temperature control in the variable conductance mode. This phenomenon happens, according to Chernysheva et al. (2007), due to two

factors: (i) decreasing of the condensation area, caused by the liquid displacement from the condenser to the compensation chamber; (ii) changing in the saturation temperature into the compensation chamber T_{11} , that influences directly in the change of the evaporation temperature, due to a complex process of heat and mass transfer. This process happens between the evaporator and the compensation chamber.

3. EXPERIMENTS DESCRIPTION

In this paper three capillary pumping systems, one LHP and two CPL, were tested in order to evaluate the thermal performance and the applicability in thermal control of microprocessors and electronic components in general. The surface temperatures at the main part of the systems, e.g. evaporator and condenser inlet and outlet, compensation chamber (LHP) and reservoir (CPL), were measured while the thermal load was varied. All systems used acetone as working fluid and a ceramic porous wick as capillary structure in the evaporator. For the heating of the capillary evaporator of the systems, electric resistors (skin heaters) were used to simulate the heating generation of microprocessors and electronic components in general. For all devices the condensers were cooled using water in forced convection.

Most porous structures used in LHP and CPL have been made of metallic material, such as nickel, titanium and stainless steel. Metallic wicks have low thermal resistance and can transfer a considerable quantity of heat from evaporation zone to the inlet liquid channel, leading to bubbles formation and blocking the liquid feeding channel. Moreover, the machining process of porous metal structures can block the external pores and hence reduce the liquid flow. In this paper, ceramic porous wicks are proposed as alternative to wicks made of metallic material for all capillary evaporators in order to minimize both problems: the bubble formation inside the liquid feed channel and the machining process of the wick. The ceramic porous wicks used have porosity of 50%, pore size of 1 to 3 μm and permeability of about $35\text{E-}15 \text{ m}^2$. All devices used acetone as working fluid.

Figures (8a) shows the LHP which has a cylindrical capillary evaporator with 10 mm of diameter and 25 mm of active length; a compensation chamber with the same diameter of the evaporator and length of 35 mm. This figure presents as well the localizations of the thermocouples on the evaporator and condenser inlets, condenser outlet, inlet of the assembly (compensation chamber and evaporator) and compensation chamber. Only the upper side of the capillary evaporator has grooves with rectangular format, as shown in Fig. (8b).

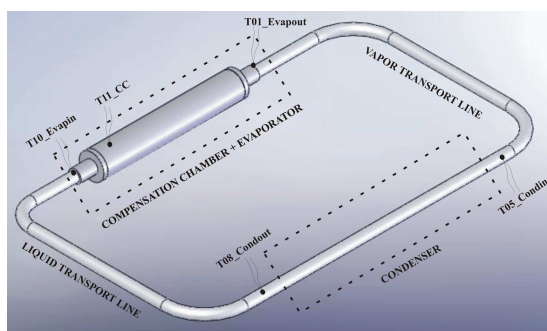


Figure 8a. Sketch of LHP and the positions of thermal resistors.

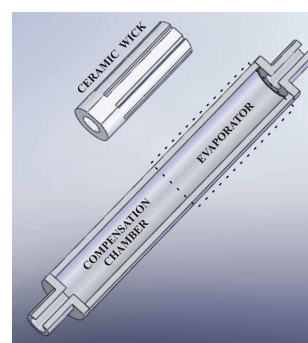


Figure 8b. Detailed sketch of the compensation chamber, capillary evaporator and ceramic porous wick assembly.

Figure (9a) depicts the LHP and the condenser box. The condenser was cooled using water in forced convection. The capillary evaporator was heated using a skin heater. Figure (9b) shows the assembly composed by the compensation chamber, the evaporator and the details of wick grooves. The assemblies of cylindrical capillary evaporators are complex because the insertion of ceramic wicks into the metallic envelope requires close contact tolerances between envelope walls and wick surface. This contact should be fit in order to avoid any vapor leak back to liquid channel. For metallic wicks this complexity increases because they require at the same time the heating of the metallic tube and cooling of the wick for the

insertion into the metallic envelop. In the ceramic wick insertion, it does not require to be cooled due to its low thermal conductivity. Only the metallic envelop should be heated.

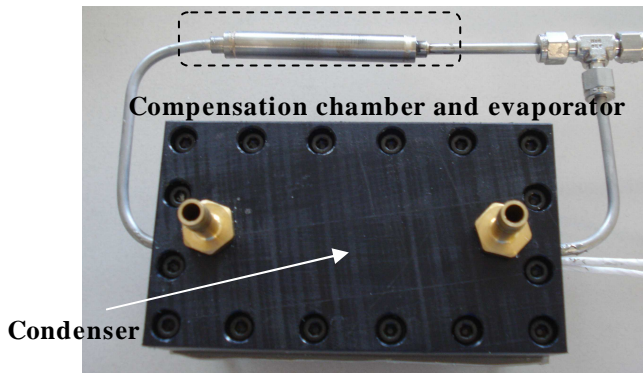


Figure 9a. View of LHP and the condenser box.

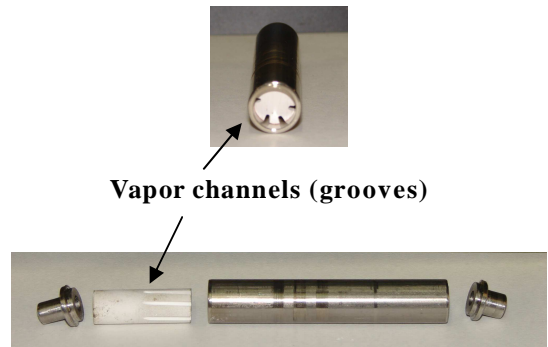


Figure 9b. View of the evaporator, the compensation chamber and the ceramic porous wick.

The Fig. (10a) shows the CPL with flat capillary evaporator which has a diameter of 30 mm and height of 10 mm. Thermocouples were used to measure the main temperatures in both CPLs. The temperature sensors in the CPL with flat evaporator were placed in evaporator inlet and outlet, reservoir and condenser inlet. The Fig. (10b) shows the CPL with cylindrical evaporator which has length of 85 mm. The temperature sensors in the CPL with cylindrical evaporator were placed in evaporator inlet and outlet, reservoir and condenser outlet. For the condenser section of both CPLs, a cooled system using water as working fluid in forced convection was used.

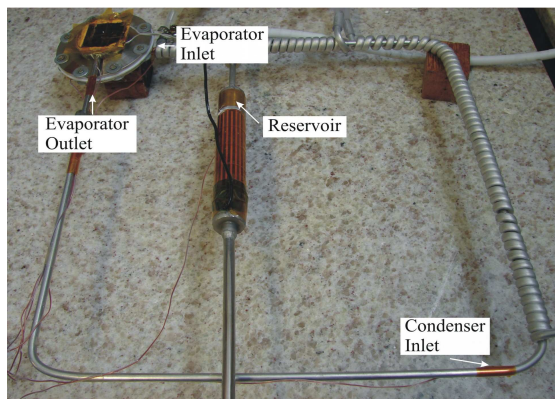


Figure 10a. CPL with flat evaporator illustration and thermocouple positions.

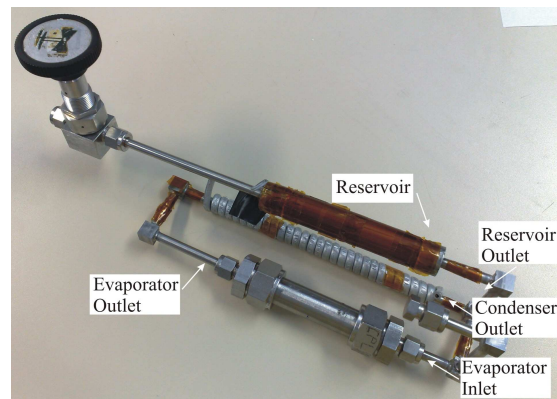


Figure 10b. CPL with cylindrical evaporator illustration and thermocouple positions.

All devices, i.e. LHP and CPL's, were successfully assembled even with the complexity of the ceramic wick insertion in evaporator envelope. The ceramic wicks presented close tolerances wherein the contact between evaporator walls and wick surface was close enough to avoid the vapor returning to liquid channel. The close tolerances of ceramic wicks were achieved with conventional machining equipment and conventional tools. This is another advantage of ceramic wick application in capillary pumping systems in comparison to metallic wicks.

4. EXPERIMENTAL RESULTS

All systems were adjusted to the orientation of interest (horizontal position) and the room temperature was measured at 23 ± 1 °C. The electrical power applied to the skin heater has been calculated by measuring the current and the voltage. The uncertainty of the measurements were evaluated for the temperature and

power input. Taking into account the accuracy of the temperature sensors (thermocouples type T) and the uncertainties of the data logger (Agilent 34970A with 20 channels), the uncertainty of the temperature measured was evaluated to be ± 1 °C. The uncertainty of the electrical power input is evaluated to be ± 0.06 W including the uncertainty of the power supply unit and the uncertainty of the data logger (Agilent N6700B).

As shown in Fig.11a, after the start up the inlet and outlet evaporator temperatures remain around 38 and 74°C, respectively, showing a very steady operation of the CPL. The applied heat load in the evaporator is effectively transported to the condenser section where it is rejected to the heat sink. The observed temperature oscillation is normal in two phase flow heat transfer. The inlet condenser temperature behavior is possible explained by existing non condensable gases or vapor bubbles in liquid channel. Despite the initial observed peaks, the temperature remains constant after a time operation of around 120 minutes. Although the successful operation, further improvements are still required in order to reduce the difference between the evaporator and sink temperatures.

The steady operation was also showed in the thermal behavior of the CPL of the Fig 11b. In this experiment the CPL evaporator with cylindrical format was undergone to heat loads changing from 10 to 30W. It is verified that even the heat load changed the vapor temperature remained 60 °C, that is, as explained before (Fig. 7a) the CPL has been working in the variable conductance model. Independently of the thermal load supplied to the CPL, the temperature was remained constant. This reflects that the evaporating mass rate increased without increasing the vaporization temperature.

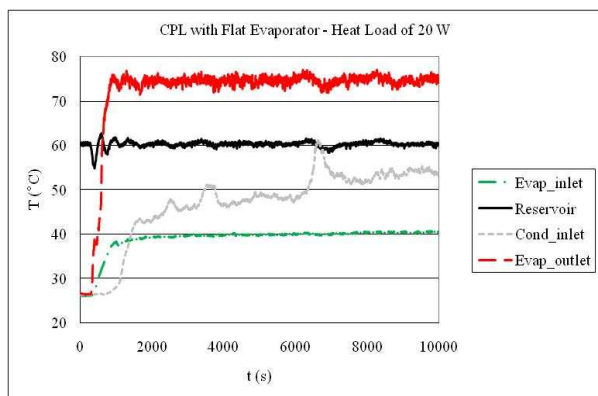


Figure 11a. Steady-state operation of the CPL with flat evaporator working with 20W of heat load.

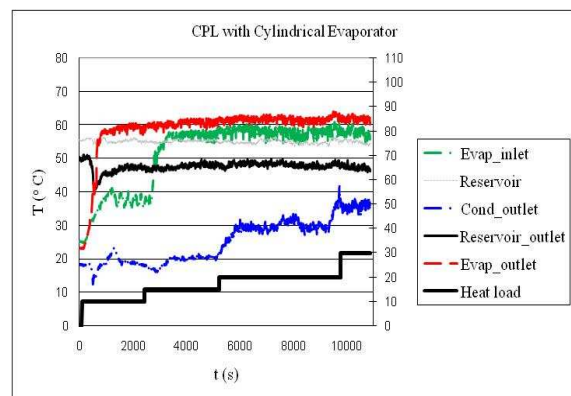


Figure 11b. Several steady-state condition in function of the heat load variation of the CPL with cylindrical evaporator.

The LHP has presented desirable behavior in the range from 5 to 25 W. Figure (12) shows the temperatures concerning the outlet evaporator, T01, inlet condenser, T05, outlet condenser, T08, inlet evaporator, T10, and the compensation chamber, T11. For a determined temperature limit of 100 °C, assumed for safety reasons, the LHP worked until 25 W power input. Unlike to capillary pumped loops, the temperature of the compensation chamber did not remain the same, changing from 29 to 51°C. The outlet evaporator temperature has been measured much higher, from 50 to 98 °C, and the temperature difference related to the heat sink temperature (20 °C), from 30 to 78 °C. This condition is determinant for a successful application of this specific LHP. Therefore, high temperature differences claim for changes in the properties of the ceramic porous wick (porosity, pore size and thermal conductivity) or improvements in the original LHP design. The thermal resistance at the interface between the porous wick and inner diameter of the evaporator should also be considered.

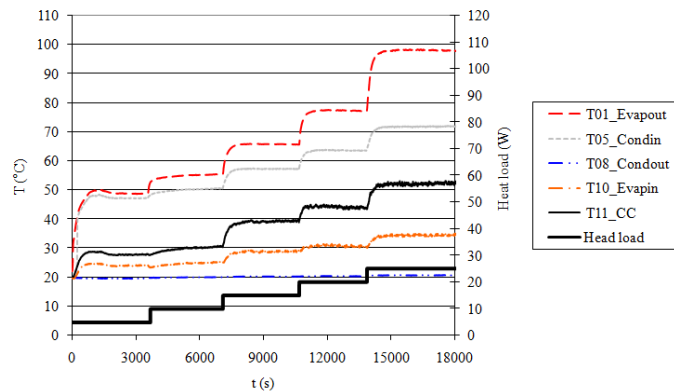


Figure 12. Steady state operation for heat load increasing at horizontal position and at heat sink temperature of 20 °C.

5. CONCLUSIONS

The proposed ceramic porous wick is a reliable alternative to be used in capillary pumping systems. The performance tests have shown a successful start up and steady state operation. No relevant problem was observed regarding the machining process of the wick and bubble formation inside the liquid feeding channel. All capillary evaporators were successfully assembled, despite of the complexity of the ceramic wick insertion in the evaporator envelope. The ceramic wick insertion does not require any cooling process to be assembled. Only the metallic envelop must be heated. A perfect fit is possible to obtain even with the use of conventional machine tools. No pore obstruction was observed.

Power inputs up to 30 W were considered for performance testing. No significant difference was observed concerning the heat transfer capacity, showing a maximum power input of 20 W (flat evaporator) and 30 W (cylindrical evaporator), in the case of CPLs, and 25 W in the case of the LHP. As a result, one can say that whatever solution here presented, the capillary evaporator meets the needs of cooling microprocessors and electronic components, in case of heat generation not exceeding 20 W.

Further researches are still required in order to reduce the operation temperature, evaluating changes related to properties of the ceramic porous wick (porosity, pore size and thermal conductivity) and improvements in the whole LHP and CPLs designs.

6. ACKNOWLEDGMENTS

The authors thank the National Council for Scientific and Technological Development (CNPq).

7. REFERENCES

- Chernysheva, M. A., Vershinin, S. V. and Maidanik, Y. F., 2007, "Operating Temperature and Distribution of a Working Fluid in LHP", *International Journal of Heat and Mass Transfer*, Vol.50, pp. 2704-2713.
- Janssen, R., Scheppokat, S., Claussen, N., "Tailor-made ceramic-based components - Advantages by reactive processing and advanced shaping techniques", *J. Eur. Ceram. Soc.*, 28, 2008, 1369-1379.
- Ku, J., 1994, "Thermodynamic Aspects of Capillary Pumped Loop Operation", *Proceedings of the 6th AIAA/ASME Joint Thermophysics and Heat Transfer Conference*, AIAA-94-2059, pp.1-11.
- Ku, J., 1999, "Operating Characteristics of Loop Heat Pipes", *Proceedings of the 29th International Conference on Environmental System*, 1999-01-2007, Denver, Colorado, USA.
- Maidanik, Y. F., Fershtater, Y. G. and Goncharov, K. A., 1991, "Capillary-pump Loop for the Systems of Thermal Regulation of Sapcecraft", *Proceedings of the 4th European Symposium on Space Environmental and Control Systems*, Florance, Italy, pp. 87-92.
- Maidanik, Y. F., 1999, "State-of-the-art of CPL and LHP Technology", *Proceedings of the 11th International Heat Pipe Conference*, Tokyo, Japan, pp. 19-30.
- Nikitkin, M. and Cullimore, B., 1998, "CPL and LHP Technologies: What are the Differences, What are the Similarities?", *SAE Paper No. 981587*.